

MnO₂@Nickel Nanocone Arrays Coated Paper Electrode for Flexible Supercapacitors

1st Min Wang

*Division of Energy and Environment
Graduate School at Shenzhen,
Tsinghua University
Shenzhen, China
wangmin17@mails.tsinghua.edu.cn*

2nd Shengyu Hu

*Division of Energy and Environment
Graduate School at Shenzhen,
Tsinghua University
Shenzhen, China
hushengyu86@sz.tsinghua.edu.cn*

3rd Songyang Su

*Division of Energy and Environment
Graduate School at Shenzhen,
Tsinghua University
Shenzhen, China
susy16@mails.tsinghua.edu.cn*

4th Xuanyu Wang

*Division of Energy and Environment
Graduate School at Shenzhen,
Tsinghua University
Shenzhen, China
ht89071@gmail.com*

5th Jiaxing Liu

*Division of Energy and Environment
Graduate School at Shenzhen,
Tsinghua University
Shenzhen, China
ljwxn@163.com*

6th Cheng Yang

*Division of Energy and Environment
Graduate School at Shenzhen,
Tsinghua University
Shenzhen, China
yang.cheng@sz.tsinghua.edu.cn*

Abstract—Flexible supercapacitors are considered as a promising candidate for power supplementation in wearable electronics due to their high power density. However, effectively fabricate flexible and low-cost supercapacitor electrodes in a big scale is still a key challenge. Herein we demonstrate a scalable fabrication method for hierarchical electrodes via metalizing air-laid paper and loading with MnO₂ as cathode active materials. To be specific, we coat a thin layer of Ni on air-laid paper by magnetron sputtering, then deposit Ni nanocone arrays (NNAs) on the Ni sputtered paper and finally deposit MnO₂ on the NNAs to obtain the NNAs@MnO₂ paper electrode. The as-prepared paper-based electrode possesses high conductivity and fine wettability, which facilitates the electrons and ions transporting through the conductive network. Additionally, this electrode provides large specific surface area with a hierarchical architecture. Thus the electrode shows high capacitance (451 F/g) and favorable cycle performance (92.9% capacity retention after cycling for 5000 times). By coupling with activated carbon (AC) coated on the NNAs conductive paper as anode, an NNAs paper-based asymmetric supercapacitor is constructed. Benefiting from the high mechanical durability and the 3D hierarchical architecture of the electrodes, the asymmetric supercapacitor exhibits excellent mechanical flexibility and high energy density (26.9 μWh/cm² at 1.08 mW/cm²). This method can be easily scaled up to produce lightweight and low-cost conductive paper electrodes, making it promising for the application of flexible supercapacitors in wearable electronics.

Keywords—flexible supercapacitor; paper electrode; MnO₂; nickel nanocone arrays

I. INTRODUCTION

Mechanically flexible energy storage components are essential for flexibilization and further miniaturization of self-powered electronic devices [1, 2]. Among all kinds of energy storage systems, supercapacitors have been regarded as promising candidates to meet the demand of portable microelectronic devices owing to the properties of excellent rate performance, high power density and long service life [3].

For practical applications, supercapacitors should be developed with excellent flexibility/deformability without sacrificing their power delivery ability and cycle life when being bended or deformed [4]. To achieve this goal, one effective way is to integrate active materials such as carbon materials, metal oxides/hydroxides and conductive polymers onto certain flexible substrates [5-7]. These substrates include

flexible metallic foils, textiles, plastic films and paper, etc. [8]. Among them, air-laid paper, made up of cellulose and polyester fibers, possesses the features of favorable water absorption property, high porosity, light-weight and excellent softness. And all of the properties mentioned ensure it as a good substrate for flexible electrodes [9]. As for conductive part, carbon materials such as carbon nanotubes (CNTs) and graphene (GN) have been previously employed to make paper electrically conductive [4, 10]. However, carbon based materials show high contact resistance when applied as current collector. In this regard, highly conductive nanostructured metal/paper-based electrode is a promising alternative to improve the charge transfer and boost the performance of supercapacitors [11]. For example, Yuan et al. prepared a highly conductive Au paper by thermal evaporation, which enhanced the specific capacity of PANI/Au/paper electrode up to 560 F/g [11]. However, there is still a key challenge to effectively fabricate flexible and low-cost supercapacitor electrodes in large scale. Therefore, it is essential to develop an effective and scalable technique to fabricate highly conductive paper-based electrodes.

Here we develop a facile strategy to fabricate conductive and flexible paper electrodes with a hierarchically porous structure. The air-laid paper was the flexible substrate, on which thin layer of Ni was coated by magnetron sputtering, then electrodeposited Ni nanocone arrays (NNAs) on the Ni coating paper to obtain a highly conductive porous paper. The NNAs was then loaded with MnO₂ by electrodeposition to obtain a hierarchical nanostructure paper electrode. The hierarchical porous structure can effectively boost the interaction between electrolyte ions and active material, which contributes to improving electrochemical performance. Benefitting from highly the conductive NNAs and hierarchical porous structure, the paper electrodes not only exhibited excellent flexibility, but also showed high electrochemical performance. As a result, a paper-based asymmetric supercapacitor device assembled with the MnO₂@NNAs cathode and activated carbon (AC) anode exhibited excellent electrochemical performances and flexibility. Combining the technologies of magnetron sputtering and electrodeposition, this method of flexible paper electrodes fabrication can be accomplished using roll-to-roll equipments for scalable production.

II. EXPERIMENTAL

A. Fabrication of NNAs coated air-laid paper

All chemicals were in analytical grade and were directly utilized without further purification. Air-laid paper (WIP-0690, 55% cellulose and 45% polyester with thickness about 350 μm) was offered by Shenzhen Vico Antistatic Technology Co., Ltd.. The NNAs paper was prepared via magnetron sputtering combined with electro-deposition process [12]. Firstly, a layer of Ni was coated onto the air-laid paper through magnetron sputtering. Then the Ni coated air-laid paper was immersed into an electro-deposition solution as the working electrode in which a commercial Ni foam was the counter electrode for NNAs preparation. The electro-deposition solution contained 0.8 M $\text{NiCl}_2 \cdot 6\text{H}_2\text{O}$, 0.6 M H_3BO_3 and 2 M NH_4Cl . This solution was kept at 60 $^\circ\text{C}$ and the pH value was 4.0 which is adjusted by 10wt% $\text{NH}_3 \cdot \text{H}_2\text{O}$ and 10wt% HCl . The samples were electrodeposited at a current density of 20 mA/cm^2 for 15 min. Subsequently, they were thoroughly cleaned in deionized water and dried.

B. Fabrication of MnO_2 @NNAs paper electrode and AC paper electrode

The cathode MnO_2 @NNAs was fabricated by electrodepositing MnO_2 on the NNAs coated air-laid papers. The deposition solution was 0.05 M $\text{Mn}(\text{Ac})_2$ aqueous and the current density is 10 mA/cm^2 , using NNAs paper as the working electrode and Ti plate as the counter electrode. For the anode, AC was mixed with acetylene black and PVDF (7:2:1 by mass ratio) in N-methyl-2-pyrrolidone and then brushed on the NNAs coated air-laid papers.

C. Materials characterization and electrochemical measurements

A scanning electron microscopy (SEM, HITACH S4800) is utilized for observing the sample microscopic morphologies. The structural information was investigated on an X-ray diffractometer (XRD, D8 Advance). The cyclic voltammetry (CV) and galvanostatic charge-discharge (GCD) profiles of samples were conducted on an electrochemical station (VMP3, Bio-Logic), and the electrochemical impedance spectroscopy (EIS) analysis was conducted (100 kHz-10 mHz at potential amplitude of 5 mV) by a CHI 610E instruments. And a Pt plate and saturated calomel electrode (SCE) were applied as the reference and counter electrodes respectively with 0.5 M Na_2SO_4 aqueous electrolyte for three-electrode system tests. The specific capacity (C) was computed from GCD curve based on the following equations:

$$C = \frac{I \cdot \Delta t}{m \cdot \Delta U} \quad (1)$$

where I is the impressed current, Δt is the discharging time and m is the active mass loading, ΔU is the electrochemical window of the discharging process. The energy and power density (E and P) were computed based on the following equations:

$$E = \frac{\int IV(t)dt}{S} \quad (2)$$

$$P = \frac{E}{\Delta t} \quad (3)$$

where I is the discharge current, $V(t)$ is the voltage, dt is the time differential, S refers to the plan area for supercapacitor device and Δt is the discharge time.

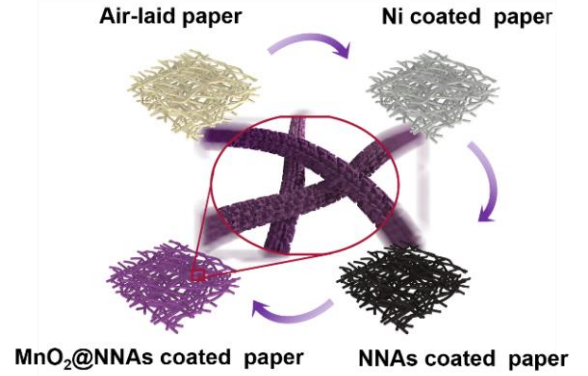


Fig. 1. Scheme of the preparation procedure for MnO_2 @NNAs coated paper electrode.

III. RESULTS AND DISCUSSIONS

Fig. 1 illustrates the preparation procedure for MnO_2 @NNAs coated paper electrode. Firstly, a layer of Ni was coated on an air-laid paper by magnetron sputtering, then the NNAs was electrodeposited on the Ni coated paper and finally MnO_2 was loaded on the NNAs to obtain the MnO_2 @NNAs paper electrode (see details in experimental section). The SEM images of Ni coated air-laid paper (Fig. 2a, 2b) illustrate that the porous air-laid paper is made up of two different fibers (cellulose and polyester fibers), ensuring good water-wettability and elasticity of the paper [10]. Fig. 2c and 2d reveal that the NNAs with a height of 500 nm are grown on the fibers homogenously without any binder. The XRD patterns in Fig. 3a confirm the existence of Ni with good crystallinity. Except the peaks from the air-laid paper substrate, the other three diffraction peaks correspond to face-centered cubic Ni (JCPDS #04-0850). After electrodeposition, MnO_2

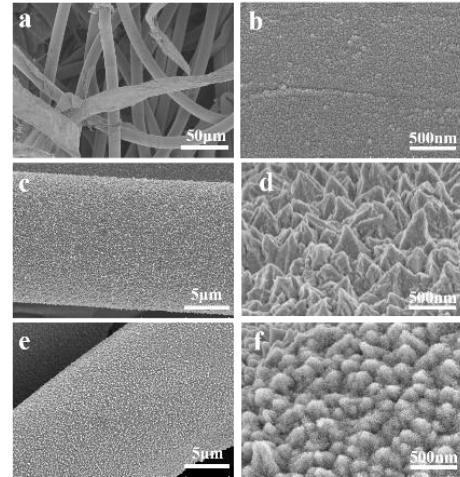


Fig. 2 SEM images of (a, b) Ni coated air-laid paper, (c, d) NNAs coated paper, and (e, f) MnO_2 structure deposited on NNAs coated paper.

is uniformly deposited on the NNAs (Fig. 2e, 2f) to form a hierarchical structure, which provides fast pathway for the transport of electrons and ions [13]. XRD pattern in Fig. 3b further confirms the existence of MnO_2 . Two additional peaks, matching well with the reference data for ϵ - MnO_2 (JCPDS #30-0820), are observed comparing to the NNAs coated paper and MnO_2 @NNAs paper electrode. The weak

and wide peaks indicate low crystallinity of the electrodeposited MnO_2 , which in good conformity to previous reports [14, 15].

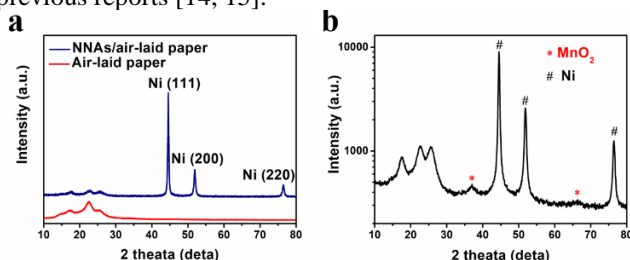


Fig. 3 (a) XRD patterns of air-laid paper and NNAs coated paper. (b) XRD pattern of MnO_2 @NNAs paper electrode.

The electrochemical properties of the MnO_2 @NNAs electrode were evaluated in a three-electrode system. The CV profiles of NNAs and MnO_2 @NNAs electrodes (Fig. 4a) suggest that the NNAs coated paper contributes to negligible capacitance to the electrode compared to the MnO_2 active materials. To assess the effect of active mass loading (MnO_2) on the electrode capacity, the specific capacitances in respect of different active mass loadings were computed and presented in Fig. 4b. Meanwhile, the electrode with mass loading of 0.17 mg/cm^2 and 0.82 mg/cm^2 show the highest gravimetric capacity (451 F/g at 1 mV/s) and the highest areal capacity (202 F/cm^2 at 1 mV/s) respectively.

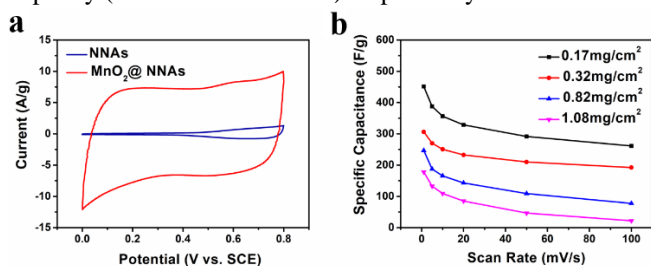


Fig. 4 (a) Characterization of CV profiles for NNAs and MnO_2 @NNAs electrodes at 50 mV/s . (b) The specific capacity as a function about scan rate for different mass loading of electrodes.

Comprehensive testings were conducted on the MnO_2 @NNAs electrode (active mass loading was 0.36 g/cm^2) for further verifying the paper electrodes electrochemical performance. Fig. 5a and 5b illustrate the characterization of CV profiles with various scanning rates and GCD profiles under different current densities for MnO_2 @NNAs electrode. The CV profiles displays rectangular even the scan rate up to 200 mV/s , showing ideal capacitive behavior. The GCD profiles are almost linear and symmetrical without observable “voltage drop (IR)”, which demonstrates the electrode owns excellent electrochemical reversibility. It is considered that the outstanding performance is due to the superior conductivity, excellent wettability and porous construction of the MnO_2 @NNAs electrode [9]. This can be verified by Nyquist plot (Fig. 5c) of the EIS for MnO_2 @NNAs tested at open-circuit potential. By fitting the impedance spectra according to electrical equivalent circuit (shown in the insert), the calculated internal resistance (R_s) and charge transfer resistance (R_{ct}) of the MnO_2 @NNAs electrode are 1.7Ω and 0.6Ω , much smaller than those of the previously reported MnO_2 -based electrodes [12, 16]. The improved conductivity benefits from the intimate direct contact of MnO_2 with the NNAs substrate, without the involvement of any polymer binder. The line at the low-frequency region approaches a vertical curve, suggesting a low diffusive resistance. It is due

to the hierarchical porous framework of the MnO_2 @NNAs accelerates the penetration of the electrolyte into the electrode and raises the interfacial area of active materials and electrolyte. Furthermore, the cycle stability of the MnO_2 @NNAs paper electrode was tested via CV measurement (Fig. 5d). CV result shows that the electrode retains 92.9% capacity after cycling for 5000 times. The above results prove the remarkable electrochemical properties of the MnO_2 @NNAs electrode for supercapacitors.

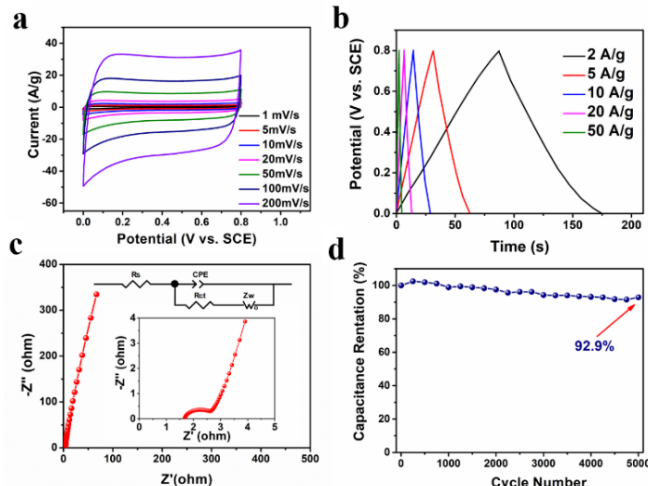


Fig. 5 (a) Characterization of CV profiles for MnO_2 @NNAs electrode. (b) GCD profiles of the MnO_2 @NNAs electrode. (c) Nyquist plots for the MnO_2 @NNAs electrode. The insets show a EIS spectra magnifying images in high-frequency region (bottom) and the corresponding equivalent circuit (top). (d) Characterization of cycle stability for the MnO_2 @NNAs electrode.

To verify the performance of the MnO_2 @NNAs paper electrode in practical applications, an asymmetric flexible supercapacitor was assembled based on MnO_2 @NNAs paper electrode and AC plated on NNAs paper as the positive and negative electrode respectively. The voltage window of AC electrode is $-0.8-0 \text{ V}$ while MnO_2 @NNAs electrode is $0-0.8 \text{ V}$ in aqueous electrolyte[17]. Therefore, the electrochemical window of the asymmetric supercapacitor can be 1.6 V in NaSO_4 aqueous electrolyte. The CV testing results for the MnO_2 @NNAs//AC supercapacitor were illustrated in Fig. 6a. Energy density of the supercapacitor can reach a value of as high as $26.9 \mu\text{Wh/cm}^2$ while the power density is 1.08 mW/cm^2 (calculated on the basis of (3) and (4) from the GCD curves in Fig. 6b). The value is higher than those of reported paper-like supercapacitors such as 3D-graphene/graphite paper ($1.24 \mu\text{Wh/cm}^2$ at $24.5 \mu\text{W/cm}^2$) [5], CNT/ MnO_2 paper ($1.8 \mu\text{Wh/cm}^2$ at maximum) [10], and MnO_2 -PPy hybrid nanofilm ($\sim 3.5 \mu\text{Wh/cm}^2$) [18].

To further evaluate the mechanical flexibility of the supercapacitor sample, bending tests were performed (Fig. 6c). While bent at various bending angles (0° , 90° or 180°), CV profiles of the supercapacitor nearly kept the constant shape, suggesting favorable flexibility[19, 20, 21]. For the electrochemical stability evaluation, CV testing (100 mV/s for 5000 cycles) was conducted (Fig. 6d). The increase of capacity during the original 400 cycles is caused by the electrolyte infiltration process in the AC electrode. Besides, the supercapacitor exhibits excellent cycle stability with 91.1% capacitance retention after cycling for 5000 times. Overall, this asymmetric supercapacitor based on the paper electrode exhibits excellent flexibility and electrochemical performance.

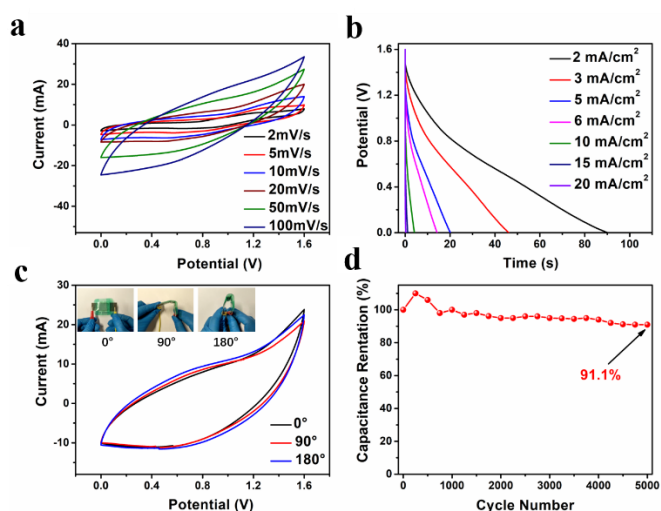


Fig. 6 (a) Characterization of CV curves for $\text{MnO}_2@NNAs//AC$ supercapacitor. (b) GCD curves of the $\text{MnO}_2@NNAs//AC$ supercapacitor. (c) Characterization of CV curves and digital photographs for the $\text{MnO}_2@NNAs//AC$ supercapacitor bent at different angles. (d) Cycle performance for the $\text{MnO}_2@NNAs//AC$ asymmetric supercapacitor.

IV. CONCLUSIONS

In conclusion, a high-performance flexible $\text{MnO}_2@NNAs$ paper electrode has been prepared by magnetron sputtering and electro-deposition technique with air-laid paper as the flexible substrate. Benefiting from the porous conductive network and hierarchical architecture, the $\text{MnO}_2@NNAs$ paper electrode exhibits good rate performance, large specific capacity, and favorable cycle performance. Based on this paper electrode, an asymmetric aqueous supercapacitor with enhanced energy density ($26.9 \mu\text{Wh}/\text{cm}^2$ at $1.08 \text{ mW}/\text{cm}^2$) has been fabricated. Meanwhile, the device shows good flexibility and electrochemical stability. Overall, this work provides an effective approach to enable the preparation of lightweight and flexible paper electrodes. By roll-to-roll technology, this low-cost method can be easily scaled up and holds great promise to apply in flexible and wearable electronics.

ACKNOWLEDGMENT

The authors thank the Local Innovative and Research Teams Project of Guangdong Pearl River Talents Program (2017BT01N111), Shenzhen Geim Graphene Center, the National Nature Science Foundation of China (Project Nos. 51578310), Guangdong Province Science and Technology Department (Project No. 2015A030306010), and Shenzhen Government (Project Nos. JCYJ20170412171430026&JSGG20170414143635496&JSGG20160607161911452) for financial supports.

REFERENCES

- [1] X. Wang, X. Lu, B. Liu, D. Chen, and Y. Tong, "Flexible energy-storage devices: design consideration and recent progress," *Adv. Mater.*, vol. 26, pp. 4763-82, July 2014.
- [2] W. Liu, C. Lu, H. Li, R. Y. Tay, and L. Sun, "Paper-based all-solid-state flexible micro-supercapacitors with ultra-high rate and rapid frequency response capabilities," *J. Math. Chem. A*, vol. 4, pp. 3754-3764, January 2016.
- [3] Y. Wang, Y. Song, and Y. Xia, "Electrochemical capacitors: mechanism, materials, systems, characterization and applications," *Chem. Soc. Rev.*, vol. 45, pp. 5925-5950, October 2016.
- [4] L. Liu, Z. Niu, L. Zhang, W. Zhou, and X. Chen, "Nanostructured graphene composite papers for highly flexible and foldable supercapacitors," *Adv. Mater.*, vol. 26, pp. 4855-62, July 2014.
- [5] A. Ramadoss, K.-Y. Yoon, M.-J. Kwak, S.-I. Kim, and S.-T. Ryu, "Fully flexible, lightweight, high performance all-solid-state supercapacitor based on 3-Dimensional-graphene/graphite-paper," *J. Power Sources*, vol. 337, pp. 159-165, January 2017.
- [6] L. Yuan, B. Yao, B. Hu, K. Huo, and W. Chen, "Polypyrrole-coated paper for flexible solid-state energy storage," *Energy Environ. Sci.*, vol. 6, p. 470, December 2013.
- [7] X. Wang, B. Liu, R. Liu, Q. Wang, and X. Hou, "Fiber-based flexible all-solid-state asymmetric supercapacitors for integrated photodetecting system," *Angew. Chem. Int. Ed.*, vol. 53, pp. 1880-1884, January 2014.
- [8] L. Dong, C. Xu, Y. Li, Z.-H. Huang, and F. Kang, "Flexible electrodes and supercapacitors for wearable energy storage: a review by category," *J. Math. Chem. A*, vol. 4, pp. 4659-4685, February 2016.
- [9] Y. Chen, K. Cai, C. Liu, H. Song, and X. Yang, "High-Performance and Breathable Polypyrrole Coated Air-Laid Paper for Flexible All-Solid-State Supercapacitors," *Adv. Funct. Mater.*, vol. 7, p. 1701247, August 2017.
- [10] L. Dong, C. Xu, Y. Li, Z. Pan, and G. Liang, "Breathable and Wearable Energy Storage Based on Highly Flexible Paper Electrodes," *Adv. Mater.*, vol. 28, pp. 9313-9319, November 2016.
- [11] L. Yuan, X. Xiao, T. Ding, J. Zhong, and X. Zhang, "Paper-based supercapacitors for self-powered nanosystems," *Angew. Chem. Int. Ed.*, vol. 51, pp. 5018-5022, May 2012.
- [12] Z. Su, C. Yang, B. Xie, Z. Lin, and Z. Zhang, "Scalable fabrication of MnO_2 nanostructure deposited on free-standing Ni nanocone arrays for ultrathin, flexible, high-performance micro-supercapacitor," *Energy Environ. Sci.*, vol. 7, pp. 2652-2659, May 2014.
- [13] Liao, J., Zou, P., Su, S., Nairan, A., Wang, Y., Hierarchical nickel nanowire@ NiCo_2S_4 nanowhisker composite arrays with a test-tube-brush-like structure for high-performance supercapacitors. *J. Math. Chem. A*, vol. 6, pp. 15284-15293, June 2018.
- [14] W. Lai, Y. Wang, Z. Lei, R. Wang, and Z. Lin, "High performance, environmentally benign and integratable Zn/MnO_2 microbatteries," *J. Math. Chem. A*, vol. 6, pp. 3933-3940, January 2018.
- [15] W. Sun, F. Wang, S. Hou, C. Yang, and X. Fan, "Zn/ MnO_2 Battery Chemistry With H^+ and Zn^{2+} Coinsertion," *J. Am. Chem. Soc.*, vol. 139, pp. 9775-9778, July 2017.
- [16] L. Li, Z. A. Hu, N. An, Y. Y. Yang, and Z. M. Li, "Facile Synthesis of MnO_2/CNTs Composite for Supercapacitor Electrodes with Long Cycle Stability," *J. Phys. Chem. C*, vol. 118, pp. 22865-22872, September 2014.
- [17] Z. Su, C. Yang, C. Xu, H. Wu, and Z. Zhang, "Co-electro-deposition of the MnO_2 -PEDOT:PSS nanostructured composite for high areal mass, flexible asymmetric supercapacitor devices," *J. Math. Chem. A*, vol. 1, p. 12432, August 2013.
- [18] C. Wang, Y. Zhan, L. Wu, Y. Li, and J. Liu, "High-voltage and high-rate symmetric supercapacitor based on MnO_2 -polypyrrole hybrid nanofilm," *Nanotechnology*, vol. 25, p. 305401, August 2014.
- [19] Tang, H., Yang, C., Lin, Z., Yang, Q., Kang, F., and Wong, C. P., Electro-spray-deposition of graphene electrodes: a simple technique to build high-performance supercapacitors[J]. *Nanoscale*, vol. 7, pp. 9133-9139, 2015 April.
- [20] Zang, X., Zhang, R., Zhen, Z., Lai, W., Yang, C. and Kang, F., Flexible, temperature-tolerant supercapacitor based on hybrid carbon film electrodes[J]. *Nano Energy*, vol. 40, pp. 224-232, 2017 August.
- [21] Wu, H., Chiang, S. W., Lin, W., Yang, C., Li, and Wong, C. P. Towards practical application of paper based printed circuits: capillarity effectively enhances conductivity of the thermoplastic electrically conductive adhesives[J]. *Sci. Rep.*, vol. 4, pp. 6275, 2014 August.